

# Electric dipole moments of superheavy elements

## A case study on copernicium

Laima Radžiūtė,<sup>1</sup> Gediminas Gaigalas,<sup>1</sup> Per Jönsson,<sup>2</sup> and Jacek Bieroń<sup>3,\*</sup>

<sup>1</sup>*Vilnius University, Institute of Theoretical Physics and Astronomy, Saulėtekio al. 3, LT-10222, Vilnius, Lithuania*

<sup>2</sup>*Group for Materials Science and Applied Mathematics, Malmö University, S-20506, Malmö, Sweden*

<sup>3</sup>*Instytut Fizyki imienia Mariana Smoluchowskiego, Uniwersytet Jagielloński, Kraków, Poland*

(Dated: June 15, 2021)

The multiconfiguration Dirac-Hartree-Fock (MCDHF) method was employed to calculate atomic electric dipole moments (EDM) of the superheavy element copernicium (Cn,  $Z = 112$ ). The EDM enhancement factors of Cn, here calculated for the first time, are about one order of magnitude larger than those of Hg. The exponential dependence of the enhancement factors on the atomic number  $Z$  along group 12 of the periodic table was derived from the EDMs of the entire homologous series,  ${}^{69}_{30}\text{Zn}$ ,  ${}^{111}_{48}\text{Cd}$ ,  ${}^{199}_{80}\text{Hg}$ ,  ${}^{285}_{112}\text{Cn}$ , and  ${}^{482}_{162}\text{Uhb}$ . These results show that superheavy elements with sufficiently long half-lives are potential candidates for EDM searches.

PACS numbers: 11.30.Er 32.10.Dk 31.15.A- 24.80.+y

### I. INTRODUCTION

The existence of a non-zero permanent electric dipole moment (EDM) of an elementary particle, or in a nondegenerate system of particles, would be one manifestation of violation of parity ( $P$ ) and time reversal ( $T$ ) symmetries [1, 2]. Violation of  $P$  symmetry has been observed in the  $\beta$ -decay of  ${}^{60}\text{Co}$  [3] followed by decay of muons [4] and pions [5]. Violation of charge and parity ( $CP$ ) symmetry has been observed in the weak decay of neutral kaons  $\text{K}^0$  [6]. Violation of  $T$  symmetry is in turn equivalent to violation of combined  $CP$  symmetry, through the combined  $CPT$  symmetry, which is considered invariant [7]. Both  $CP$  and  $T$  symmetry violations have been observed in the neutral kaon system [8], although direct  $T$  symmetry violation has been disputed [9, 10]. More recently a direct observation of the  $T$  symmetry violation in the  $B$  meson system has been reported [11]. The violations of  $P$ ,  $C$ ,  $CP$ , and  $T$  symmetries are predicted by the Standard Model (SM) of particle physics [12, 13]. However, the SM leaves several issues unexplained, such as the origin of baryogenesis, the mass hierarchy of fundamental particles, the number of particle generations, the matter-antimatter-asymmetry observed in the universe, and the nature of the dark matter. These and other issues are addressed within a large number of extensions of the present version of the SM. Several of these extensions predict EDMs induced by the  $P$  and  $T$  violating interactions and also EDMs of the fundamental particles significantly larger than the values predicted by the SM itself. The predictions can be tested, and searches for permanent electric dipole moment are underway presently in various systems — neutrons [14], electrons in para- and diamagnetic atoms [15, 16], molecules [17, 18], and other species [1, 19, 20]. The experimental searches have

not yet detected a non-zero EDM, but they continue to improve the limits on EDMs of individual elementary particles, as well as limits on  $CP$ -violating interactions, parametrized by the coupling constants  $C_T$  and  $C_P$  (see references [1, 21, 22] for details, and the Table II in the reference [23] for a summary).

The primary objective of the present paper is the calculation of EDM for the superheavy element copernicium [24, 25]. We evaluated the contributions to the atomic EDM induced by four mechanisms [19]: tensor-pseudotensor (TPT) and pseudoscalar-scalar (PSS) interactions, nuclear Schiff moment (NSM), and electron electric dipole moment interaction with the nuclear magnetic field (eEDM). In each case we show that there is an order of magnitude increase of atomic EDM between mercury and copernicium. The second objective of the present paper is to derive the  $Z$ -dependence of atomic EDM. We show that numerical EDM results are consistent with an exponential  $Z$ -dependence along the group 12 elements.

### II. MCDHF THEORY

We used the MCDHF approach to generate numerical representations of atomic wave functions. An atomic state function  $\Psi(\gamma P J M_J)$  is obtained as a linear combination of configuration state functions  $\Phi(\gamma_r P J M_J)$  that are eigenfunctions of the parity  $P$ , and total angular momentum operators  $J^2$  and  $M_J$ :

$$\Psi(\gamma P J M_J) = \sum_r c_r \Phi(\gamma_r P J M_J). \quad (1)$$

The multiconfiguration energy functional was based on the Dirac-Coulomb Hamiltonian, given (in a.u.) by

$$\hat{H}_{DC} = \sum_{j=1}^N \left( c\alpha_j \cdot \mathbf{p}_j + (\beta_j - 1)c^2 + V(r_j) \right) + \sum_{j < k}^N \frac{1}{r_{jk}}, \quad (2)$$

\*Jacek.Bieron@uj.edu.pl

where  $\alpha$  and  $\beta$  are the Dirac matrices, and  $\mathbf{p}$  is the momentum operator. The electrostatic electron-nucleus interaction,  $V(r_j)$ , was generated from a nuclear charge density distribution  $\rho(r)$ , which was approximated by the normalized to  $Z$  two-component Fermi function [26]

$$\rho(r) = \frac{\rho_0}{1 + e^{(r-b)/a}}, \quad (3)$$

where  $a$  and  $b$  depend on the mass of the isotope. The effects of the Breit interaction, as well as QED effects, were neglected, since they are expected to be small at the level of accuracy attainable in the present calculations.

### III. MCDHF WAVE FUNCTIONS

We calculated the wave functions of five diamagnetic atoms of group 12, and subsequently the EDMs in the ground states of the entire homologous series,  $^{69}_{30}\text{Zn}$ ,  $^{111}_{48}\text{Cd}$ ,  $^{199}_{80}\text{Hg}$ ,  $^{285}_{112}\text{Cn}$ , and  $^{482}_{162}\text{Uhb}$ . The numerical representations of the wave functions were generated with the relativistic atomic structure package GRASP2K [27], based on the multiconfiguration Dirac-Hartree-Fock (MCDHF) method [26, 28–32]. Electron correlation effects were evaluated with methods described in our previous papers [33–36]. Core-valence and valence-valence correlations were included by allowing single and restricted double substitutions to five sets of virtual orbitals. The full description of numerical methods, virtual orbital sets, electron substitutions, and other details of the computations can be found in [33]. Compared with [33] the double electron substitutions were however extended from the  $nsnp$  to the  $(n-1)dnsnp$  shells in the present paper (see section V below for details).

### IV. EDM CALCULATIONS

An atomic EDM can be written as a sum over states (equation (4) in reference [33]):

$$d^{int} = 2 \sum_i \frac{\langle 0 | \hat{D}_z | i \rangle \langle i | \hat{H}_{int} | 0 \rangle}{E_0 - E_i}, \quad (4)$$

where  $|0\rangle$  represents the ground state  $|\Psi(\gamma P J M_J)\rangle$  of a closed-shell atom from the group 12, with  $J = 0$  and even parity. The summation runs over excited states  $|\Psi(\gamma_i(-P) J_i M_{J_i})\rangle$ , with  $J_i = 1$  and odd parity. A calculation of an atomic EDM requires evaluation of the matrix elements of the static dipole  $\hat{D}_z$ , and the matrix elements of the  $\hat{H}_{int}$  interactions, which induce an EDM in an atom [37]. In order to perform these calculations the GRASP2K package was extended. The extension includes programs for matrix element calculations, based on spin-angular integration [37]. Here  $\hat{H}_{int}$  represents one of the four interactions mentioned in the section I above,  $E_0$  and  $E_i$  are energies of ground and excited

states, respectively. The full description of the EDM theory underlying the presents calculations can be found in reference [33], and in references therein.

The summation in equation (4) involves an infinite number of bound states, as well as contributions from the continuum spectrum. The sum over the bound spectrum was evaluated by explicitly calculating contributions from the lowest five odd states of each symmetry using numerical wave functions. Then the method of 'Riemann zeta tail', described in reference [33], was applied to sum up the contribution from the remaining bound states. To this end we showed that a summation over a Rydberg series, when extrapolated to large values of the principal quantum number  $n$  of the running electron (and where the energy denominator saturates at the ionisation energy) converges to the Riemann zeta function. The explicit numerical summation accounts for 98 percent of the whole sum, and we evaluated the upper bound on the rest (the infinite tail) of the sum by exploiting regularities of the Rydberg series. The relative correction, i.e. the total contribution from the trailing terms (called Riemann zeta tail) divided by the total contribution from the five leading terms, is of the order of 1.5 percent for mercury  $^{199}\text{Hg}$ , and below 2 percent for copernicium  $^{285}\text{Cn}$ . We neglected the Riemann zeta tail correction for the other three elements ( $^{69}\text{Zn}$ ,  $^{111}\text{Cd}$ ,  $^{482}\text{Uhb}$ ).

The contribution from the continuum is difficult to estimate, since it is partially accounted for by the virtual set [38] In the present paper we computed only the contribution of the bound states. We neglected the explicit summation over continuum, and assumed that the continuum spectrum contribution were included into the error budget. The evaluation of the sum over the continuum part of the spectrum could in principle be carried out either fully numerically [39], or again by an extrapolation, based on the fact, that the oscillator strength density is continuous across the ionization threshold [40], and above mentioned regularities carry over to the continuum spectrum.

The electronic matrix elements in equation (4) are not isotope-specific. However, the atomic wave functions do exhibit a (rather weak) dependence on the atomic mass of the element of interest, through the nuclear electrostatic potential, which depends on the nuclear charge density distribution, which in turn depends on the nuclear mass number, through the equation (3). Therefore, all numerical results in Tables I, II, III, and IV were obtained for specific isotopes, such as  $^{199}\text{Hg}$  and  $^{285}\text{Cn}$ , and they do exhibit a (negligibly weak) dependence on atomic masses.

### V. MERCURY

The calculations for  $^{199}\text{Hg}$  were performed in a similar manner as those presented in our previous paper [33]. The results from DF and from calculations with the first two layers of virtual orbitals (i.e. the first three lines in

TABLE I: TPT interaction contributions to EDM in different virtual sets, in units ( $10^{-20} C_T \langle \sigma_A \rangle |e| \text{ cm}$ ), for  $^{69}\text{Zn}$ ,  $^{111}\text{Cd}$ ,  $^{199}\text{Hg}$ , and  $^{285}\text{Cn}$ , compared with data from other methods. See text for explanations and details.

VOS	$^{69}\text{Zn}$		$^{111}\text{Cd}$		$^{199}\text{Hg}$		$^{285}\text{Cn}$		
	Th	SE	Th	SE	Th	SE	Th	Th2	Th3
DF	-0.07	-0.07	-0.35	-0.36	-7.29	-6.15	-59.86	-61.50	-66.66
1	-0.08	-0.09	-0.39	-0.45	-4.13	-4.86	-48.53	-50.95	-53.95
2	-0.09	-0.11	-0.45	-0.54	-4.66	-5.23	-58.38	-58.92	-62.96
3	-0.10	-0.12	-0.47	-0.57	-4.84	-5.53	-59.31	-64.53	-68.76
4	-0.10	-0.12	-0.48	-0.59	-4.79	-5.64	-57.67	-61.04	-65.26
5	-0.11	-0.12	-0.49	-0.60	-4.84	-5.64	-57.51	-60.75	-64.98
Ref. [41](DHF)							-2.4		
Ref. [42](DHF)							-2.0		
Ref. [41](CI+MBPT)							-5.12		
Ref. [41](RPA)							-5.89		
Ref. [42](RPA)							-6.0		
Ref. [43](CPHF)							-6.75		
Ref. [44](CCSD)							-4.3		

Tables I, II, III, and IV) are in fact identical with the results published in [33]. Further calculations differ in the scope of the double electron substitutions, which were extended from  $6s6p$  to  $5d6s6p$  shells. The results of the

TABLE II: PSS interaction contributions to EDM in different virtual sets, in units ( $10^{-23} C_P \langle \sigma_A \rangle |e| \text{ cm}$ ), for  $^{69}\text{Zn}$ ,  $^{111}\text{Cd}$ ,  $^{199}\text{Hg}$ , and  $^{285}\text{Cn}$ , compared with data from other methods. See text for explanations and details.

VOS	$^{69}\text{Zn}$		$^{111}\text{Cd}$		$^{199}\text{Hg}$		$^{285}\text{Cn}$		
	Th	SE	Th	SE	Th	SE	Th	Th2	Th3
DF	-0.13	-0.14	-0.94	-0.96	-25.47	-21.49	-199.52	-252.66	-274.11
1	-0.15	-0.17	-1.05	-1.21	-14.54	-17.16	-199.52	-209.13	-221.73
2	-0.19	-0.23	-1.19	-1.46	-16.38	-18.39	-240.22	-242.15	-259.07
3	-0.20	-0.24	-1.25	-1.53	-17.01	-19.47	-244.96	-266.95	-284.65
4	-0.20	-0.24	-1.28	-1.58	-16.84	-19.84	-237.56	-251.33	-268.95
5	-0.22	-0.24	-1.30	-1.60	-17.02	-19.85	-236.88	-250.07	-267.78
Ref. [41](DHF)							-8.7		
Ref. [41](CI+MBPT)							-18.4		
Ref. [41](RPA)							-20.7		

calculations are presented in Tables I, II, III, and IV. The number of virtual orbital sets (VOS) is listed in the first column of each table (see chapter III of reference [33] for definitions and for the details of the calculations). The line marked 'DF' (Dirac-Fock) in the VOS column represents the lowest-order approximation, with zero sets of virtual orbitals. It should be noted that the values in the Tables marked 'DF' and 'DHF' are not equivalent. Those marked 'DF' were obtained in the present calculations with only the two lowest excited states included in the summation in equation (4). The results marked 'DHF', obtained with MBPT methods, involved summation over the entire spectrum of virtual orbitals, using various methods to construct the virtual orbital set [41, 42, 47]. Neither 'DF' nor 'DHF' include electron correlation effects and therefore they are relevant only

TABLE III: Schiff moment contributions to atomic EDM in different virtual sets, in units ( $10^{-17} [S/(|e| \text{ fm}^3)] |e| \text{ cm}$ ), for  $^{69}\text{Zn}$ ,  $^{111}\text{Cd}$ ,  $^{199}\text{Hg}$ , and  $^{285}\text{Cn}$ , compared with data from other methods. See text for explanations and details.

VOS	$^{69}\text{Zn}$		$^{111}\text{Cd}$		$^{199}\text{Hg}$		$^{285}\text{Cn}$		
	Th	SE	Th	SE	Th	SE	Th	Th2	Th3
DF	-0.04	-0.04	-0.18	-0.19	-2.86	-2.46	-17.73	-17.26	-19.53
1	-0.05	-0.06	-0.21	-0.26	-1.95	-2.45	-13.64	-12.96	-14.53
2	-0.06	-0.07	-0.25	-0.32	-2.11	-2.42	-17.05	-15.96	-17.78
3	-0.06	-0.08	-0.27	-0.34	-2.21	-2.58	-20.09	-22.66	-24.58
4	-0.06	-0.08	-0.28	-0.35	-2.19	-2.62	-17.75	-18.02	-19.95
5	-0.07	-0.08	-0.28	-0.35	-2.22	-2.63	-17.62	-17.77	-19.71
Ref. [41](DHF)							-1.2		
Ref. [41](CI+MBPT)							-2.63		
Ref. [41](RPA)							-2.99		
Ref. [45](CI+MBPT)							-2.8		
Ref. [46](TDHF)							-2.97		
Ref. [44](CCSD)							-5.07		

TABLE IV: Contributions of electron EDM interaction with magnetic field of nucleus, to atomic EDM in different virtual sets, in units ( $d_e \times 10^{-4}$ ), for  $^{69}\text{Zn}$ ,  $^{111}\text{Cd}$ ,  $^{199}\text{Hg}$ , and  $^{285}\text{Cn}$ , compared with data from other methods. See text for explanations and details.

VOS	$^{69}\text{Zn}$		$^{111}\text{Cd}$		$^{199}\text{Hg}$		$^{285}\text{Cn}$		
	Th	SE	Th	SE	Th	SE	Th	Th2	Th3
DF	0.13	0.14	-0.62	-0.63	16.04	13.41	314.03	324.40	350.09
1	0.11	0.09	-0.64	-0.71	8.47	9.58	254.78	269.22	283.51
2	0.13	0.13	-0.69	-0.81	9.63	10.64	305.55	309.48	328.86
3	0.14	0.14	-0.72	-0.85	9.99	11.30	305.13	329.18	349.47
4	0.14	0.14	-0.73	-0.87	9.90	11.53	300.39	318.41	338.60
5	0.13	0.11	-0.75	-0.88	10.00	11.50	299.67	317.11	337.40
Ref. [41](DHF)							4.9		
Ref. [47](DHF)							5.1		
Ref. [41](CI+MBPT)							10.7		
Ref. [41](RPA)							12.3		
Ref. [47](RPA)							13		

for the purpose of evaluating the contributions of electron correlation for the expectation values of interest. A larger number of VOS represents in principle a better approximations of the wave function. The line marked '5' in the VOS column represents the final approximation, with five sets of virtual orbitals (MCDHF-VOS.5, represented by red circles in Figure 2). The difference between VOS.4 and VOS.5 may (cautiously) be taken as an indication of accuracy. For each element the calculated values of the energy denominators in equation (4) were used to evaluate the atomic EDMs. These fully theoretical EDM values are marked 'Th' in Tables I, II, III, and IV. Semiempirical EDM values (marked 'SE' in the Tables) were also evaluated for  $^{69}\text{Zn}$ ,  $^{111}\text{Cd}$ , and  $^{199}\text{Hg}$ , with the energy denominators taken from the NIST database [48]. Level identifications were made with the atomic state functions transformed from  $jj$ -coupling to  $LSJ$  coupling scheme, using the methods developed in [49, 50].

## VI. COPERNICIUM

Three different sets of energy denominators for  $^{285}\text{Cn}$  were used. Those from the present calculations are marked 'Th'. For comparison purposes we computed also the EDMs with the energy denominators taken from two other theoretical papers [51, 52]. The results in column marked 'Th2' were obtained with the energy denominators taken from [51], who used a large-scale MCDHF method. The authors of [51] evaluated also the ionization limit of copernicium and their calculated ionization energy was used in our evaluation of EDMs for those levels which were not reported in [51]. The energy denominators in the columns marked 'Th3' were taken from reference [52], where the energy spectrum was computed with two methods: CI+MBPT and CI. We gave priority to the CI+MBPT results; the CI results were used when CI+MBPT data were not available; for the remaining levels the energy denominators were replaced by the calculated ground state ionization energy. The accuracy of our calculated energy values, as well as those from the references [51] and [52], is better than 20% for the lowest excited levels of mercury.

The mass number 285 for the element Cn was chosen due to predictions that heavier isotopes are more stable than the lighter ones [53, 54]. The lifetimes of several known isotopes of Cn are counted in minutes [55], which make them amenable to atom traps, and subsequent spectroscopy. It is predicted that still heavier isotopes of Cn, with mass numbers in the range 290–294, may have half-lives counted in years [54].

We observed a similar pattern of contributions from individual electronic states, as described in [33]. The triplet  $6snp\ ^3P_1$  and the singlet  $6snp\ ^1P_1$  states are the dominant contributors to atomic EDM in the  $^{199}\text{Hg}$  spectrum. For the  $^{285}\text{Cn}$  case the dominant contributions arise from the lowest states of  $^{1,3}P_1$  symmetries, i.e.  $7snp\ ^1P_1$ ,  $7snp\ ^3P_1$ . Altogether they contribute in excess of 98% of the total EDM. The remaining Rydberg states contribute less than 2 percent. Instead of an explicit error analysis for the calculations of EDM for  $^{285}\text{Cn}$  we applied a comparison with mercury. Estimates of the magnitudes of EDMs induced by the TPT, PSS, NSM, and eEDM mechanisms in mercury, have been performed with several theoretical methods [41, 43, 44, 46]. With one or two exceptions [44, 56], they all agree within reasonable error bounds — of the order of 10–20 percent [33]. The results of the MCDHF calculations for mercury, both in present paper as well as in [33], are well within these bounds. We expect that the present calculations for  $^{285}\text{Cn}$ , performed with the same MCDHF model as those for  $^{199}\text{Hg}$ , would also fit within error bounds of similar size.

## VII. UNHEXBIUM

In addition to the calculations described above we have done uncorrelated DF calculations for  $^{482}\text{Uhb}$  and

for  $^9_4\text{Be}$ . There are several theoretical predictions [57–59] which suggest that the heaviest homologue in the Zn-Cd-Hg-Cn-Uxx group would not be element E162 (Unhexbium), but E164 (Unhexquadium). Due to a very large spin-orbit splitting of the  $8p$  shell, the relativistic  $8p_{1/2}$  shell becomes occupied before the  $7d$  shell is filled [59]. Therefore, at the end of transition metals in the row eight of the periodic table appears the element E164, with the ground configuration  $[\text{Cn}]5g^{18}6f^{14}7d^{10}7p^68s^28p^2$ , with all inner shells closed, and with two electrons in the  $8p_{1/2}$  shell (the  $8p_{1/2}$  shell is, in fact, also closed). However, the presence of the  $8p$  shell would complicate the calculations of EDMs, and, more importantly, it would complicate comparisons along the homologous series. Therefore we have deliberately chosen a (doubly artificial) isotope  $^{482}_{162}\text{Uhb}$ , of element E162, with electron configuration  $[\text{Cn}]5g^{18}6f^{14}7d^{10}7p^68s^2$ .

## VIII. Z-DEPENDENCE

Atomic properties depend in various ways on the atomic number  $Z$ , both in isoelectronic sequences [60–63], as well as along homologous sequences [64, 65]. In many cases approximate analytic relations were derived [60, 63–65], and several atomic observables exhibit a polynomial or power dependencies on the atomic number  $Z$ .

Atomic enhancement factors of the  $PT$ -odd interactions in neutral atoms scale with nuclear charge as  $d_{at} \sim \alpha^2 Z^3$ . The factor  $Z^3$  arises from an estimate of the strength of the electric field in the vicinity of an atomic nucleus (see chapter 6.2 of the reference [1]), but it has been pointed out that on top of the  $Z^3$  enhancement of the  $PT$ -odd interaction there is another enhancement factor, arising from relativistic contraction of the electronic wave function [1, 66–71].

$$K_r \approx \left( \frac{\Gamma(3)}{\Gamma(2\gamma + 1)} \right)^2 \left( \frac{2Zr_N}{a_0} \right)^{2\gamma-2}. \quad (5)$$

$Z$ -dependence of atomic EDMs induced by the  $(P, T)$ -odd  $\hat{H}_{int}$  interactions is governed by the  $Z$ -dependence of three factors in equation (4): matrix element of the  $(P, T)$ -odd  $\hat{H}_{int}$  operator, matrix element of the electric dipole  $\hat{D}_z$  operator, and the energy denominator  $(E_0 - E_i)$ . The matrix elements of the electric dipole  $\hat{D}_z$  operator are constrained by the Thomas-Reiche-Kuhn rule. In case of the elements of group 12 they are further constrained by the Wigner-Kirkwood sum rule (see chapter 14 of the reference [64]). The two lines,  $ns^2\ ^1S_0 - nsnp\ ^3P_1$  and  $ns^2\ ^1S_0 - nsnp\ ^1P_1$ , dominate the Wigner-Kirkwood sum in all five elements, making the matrix element of  $\hat{D}_z$  approximately constant along the homologous series. Transition energy denominators in the equation (4) do not depend on  $Z$  along the homologous series [65], except for small variations due to shell con-

tractions, shell rearrangements, etc (excluding the Uhb element, with its large spin-orbit splitting mentioned in the section VI above).

Therefore, the dominant role in establishing the  $Z$ -dependence of atomic EDMs along the homologous sequence is taken by the  $\hat{H}_{int}$  operators. Following the analysis in chapter 8 of the reference [1], it can be shown that in the vicinity of a point-like atomic nucleus the large  $P_{n\kappa}$  and small  $Q_{n\kappa}$  radial components of a one-electron wave function may be expressed as

$$P_{n\kappa}(r) = \frac{\kappa}{|\kappa|} (\kappa - \gamma) \left( \frac{Z}{a_0^3 \nu^3} \right)^{1/2} \frac{2}{\Gamma(2\gamma + 1)} \left( \frac{a_0}{2Zr} \right)^{1-\gamma} \quad (6)$$

$$Q_{n\kappa}(r) = \frac{\kappa}{|\kappa|} (Z\alpha) \left( \frac{Z}{a_0^3 \nu^3} \right)^{1/2} \frac{2}{\Gamma(2\gamma + 1)} \left( \frac{a_0}{2Zr} \right)^{1-\gamma}, \quad (7)$$

where  $\kappa$  is the angular momentum quantum number,  $\gamma^2 = \kappa^2 - \alpha^2 Z^2$ ,  $\alpha$  is the fine structure constant,  $\nu^3$  is the effective principal quantum number, and  $a_0$  is the Bohr radius. The radial integrals involved in the calculations of matrix elements of  $\hat{H}_{int}$  include the integrands of the combinations of the large  $P_{n\kappa}$  and small  $Q_{n\kappa}$  radial components, of the type  $(P_a P_b \pm Q_a Q_b)$  or  $(P_a Q_b \pm P_b Q_a)$ . All these integrals include factors in the integrands which effectively cut off the integrals outside the nucleus [33], and eventually  $Z$ -dependence of the atomic EDM in the form

$$d_{at} \sim \left( \frac{Z^k}{a_0^3 \nu^3} \right) \left( \frac{2}{\Gamma(2\gamma + 1)} \right)^2 \left( \frac{2Zr_N}{a_0} \right)^{2\gamma-2} \quad (8)$$

is obtained, where  $k$  depends on a particular form of the integrand and where  $r_N$  is the effective cut off radius. The right hand side of the equation (8) is displayed in Fig. 1. All four combinations ( $P_a P_b$ ,  $Q_a Q_b$ ,  $P_a Q_b$ , and  $P_b Q_a$ ) of the one-electron wave function factors from equations (6) and (7) are represented as functions of atomic number  $Z$ . The index  $a$  represents  $ns_{1/2}$  orbitals, the index  $b$  represents  $np_{3/2}$  orbitals. The nuclear radius  $r_N$  has been computed using  $r_N = r_0 \cdot A^{1/3}$ , where  $r_0 = 1.25$  fm. The relation of atomic mass  $A$  to atomic number  $Z$  has been evaluated from the neutrons to protons ratio  $N/Z = 1 + A^{2/3} a_C / 2a_A$ , derived from the Bethe-Weizsäcker formula [72], with  $a_C = 0.711$  and  $a_A = 23.7$ . The empty circles in the Fig. 1 show positions of the four elements (Zn, Cd, Hg, Cn) considered in this paper. Neglecting a weak  $Z$ -dependence through the gamma function  $2/\Gamma(2\gamma + 1)$ , for small values of  $Z$  the polynomial factor  $Z^k$  determines the functional form of the dependence on  $Z$  while for large values of  $Z$  the exponential factor  $(2Zr_N)^{2\gamma-2}$  takes over. It can be shown numerically, as can be seen in the Figure 1, that the polynomial  $Z^k$  shape dominates up to about  $Z = 60$ , then in the range  $60 < Z < 120$  the function  $d_{at}(Z)$  is approximately exponential, and eventually the approximation breaks down, because the analytic approximation

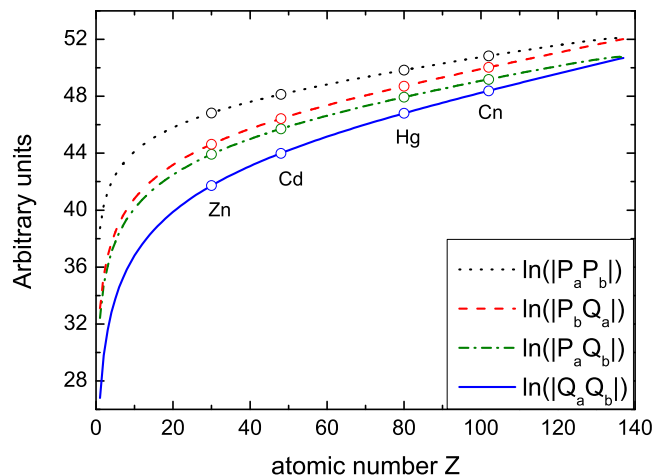


FIG. 1: (Color online):  $Z$ -dependence of the atomic EDM. The right hand side of the equation (8), calculated from (absolute values of) one-electron wave function factors  $P_a P_b$ ,  $Q_a Q_b$ ,  $P_a Q_b$ , and  $P_b Q_a$ . The factors were generated from the equations (6) and (7), and evaluated at  $r = r_N$ , as functions of atomic number  $Z$ . See text for details.

in equations 6 and 7 is valid only within the atomic number  $Z$  range, where bound solutions of the Dirac equation exist ( $Z \leq 137$  for point-like nuclei).

The analysis above has been made under the assumption of a point-like Coulomb field in the Dirac radial equation. The finite sizes of nuclei entered only when the equation (8) was evaluated. For extended nuclei the solution of the Dirac equation depends on the specific form of the nuclear charge distribution [32, 73, 74]. Flambaum and Ginges [71], and Dzuba et al [21] assumed uniform distribution of the electric charge inside a sphere (with the normalization factors from [70]), and obtained enhancement factors of a similar form as in equations (5) and (8), for angular symmetries  $s_{1/2}$ ,  $p_{1/2}$ , and  $p_{3/2}$ .

In the present paper the numerical calculations for the homologous series of the group 12 of the periodic table ( $^{69}_{30}\text{Zn}$ ,  $^{111}_{48}\text{Cd}$ ,  $^{199}_{80}\text{Hg}$ ,  $^{285}_{112}\text{Cn}$ , and  $^{482}_{162}\text{Uhb}$ ) were performed with extended nuclear model (3), for which bound solutions of the Dirac-Fock equations exist up to  $Z = 173$  [75]. The dependence of EDMs on atomic number  $Z$  along group 12 of the periodic table is presented in Fig. 2. The red circles represent our final results, calculated within the MCDHF-VOS.5 electron correlation model described above. The blue pluses represent the uncorrelated DF results. The green plus in the upper right corner represents the EDM value for Uhb. Due to very large spin-orbit splitting of the  $8p$  shell, (see section VI above), the Uhb energy denominators are distinctively different from those of other members of the homologous series. To compensate for this splitting, we also computed the EDMs for Uhb with energy denominators taken from Cn. The latter value is represented by the square in Fig. 2. The solid line is fitted to the four (Zn, Cd, Hg, Cn) final results. The dashed line is fit-

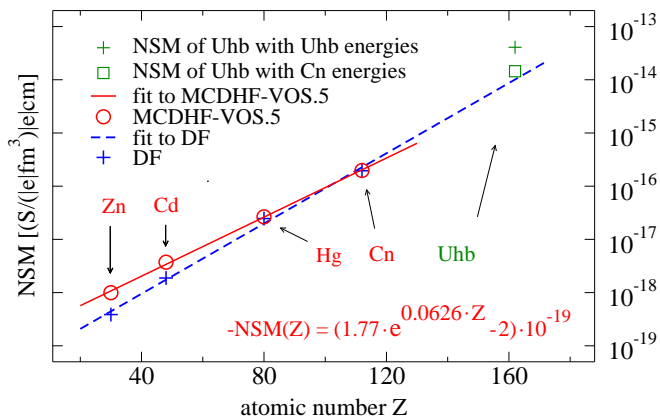


FIG. 2: (Color online): Atomic EDM (absolute values) induced by the NSM as a function of atomic number  $Z$ . Red circles = MCDHF-VOS.5 results with 5 virtual orbital sets. Blue pluses = uncorrelated DF results (0 sets). The lines are exponential functions fitted to the four points, representing Zn, Cd, Hg, and Cn. Solid red line = fit to MCDHF-VOS.5 results. Dashed blue line = fit to uncorrelated DF results. The lines are extrapolated beyond  $Z = 112$ . The two symbols in the upper right corner represent Uhb (excluded from the fitting). Green plus = DF result for Uhb with calculated Uhb energy denominators. Green square = DF result for Uhb with energy denominators taken from Cn. The sizes of circles represent approximately the relative accuracy of the MCDHF-VOS.5 calculations. See text for details.

ted to the four uncorrelated DF results. The Uhb results were excluded from the fitting. The regression analysis yields the following relations:

$$\begin{aligned}
 d^{TPT} &= [-1.22(8) \cdot e^{0.0766(6) \cdot Z} - 5(6)] \cdot 10^{-22} \\
 d^{PSS} &= [-30(1) \cdot e^{0.0813(3) \cdot Z} - 8.54(1)] \cdot 10^{-26} \\
 d^{NSM} &= [-1.77(7) \cdot e^{0.0626(3) \cdot Z} + 2(2)] \cdot 10^{-19} \\
 d^{eEDM}/\mu &= [2.74(8) \cdot e^{0.0841(2) \cdot Z} - 15(9)] \cdot 10^{-6}
 \end{aligned} \quad (9)$$

where the numbers in parentheses represent RMSE deviations. The third line of the equation (9) is displayed in Fig. 2.

Similar regression analysis can be done for the semi-analytic relations presented for the point-nucleus case in the equation (8) and in the Fig. 1, but restricted to the range of atomic numbers  $30 \leq Z \leq 112$ , covered by the four elements (Zn, Cd, Hg, Cn) considered in this paper. The analysis yields  $d^{PSS} \sim e^{0.017 \cdot Z}$  and  $d^{NSM} \sim e^{0.022 \cdot Z}$ , somewhat smaller exponents than those presented in the equation (9).

The deviation of the EDM value for the element E162 from the fitted function in Figure 2 may be explained by several possible mechanisms: rearrangements of the valence shells, i.e. relativistic contraction of the  $8s$  and  $8p_{1/2}$  shells, which results in the above mentioned large spin-orbit splitting of the  $8p$  shell; variation of transition energy denominators, induced by shell rearrangements; contribution of QED effects, which could be quite sizeable near the end of the periodic table at  $Z = 173$  [75, 76].

However, the most likely explanation is the breakdown of the exponential approximation near the end of the periodic table. The analytic approximation in equations 6 and 7 is valid only within the atomic number  $Z$  range, where bound solutions of the Dirac equation exist ( $Z \leq 137$  for point-like nuclei,  $Z \leq 173$  for extended nuclei). The element E162 is close to the end of the periodic table at  $Z = 173$ , where determination of a numerical wave function, even at the Dirac-Fock level, may be problematic or impossible, and one might expect a question whether perturbation theory still works in QED for elements close to  $Z = 173$  [75].

At very short distances  $Z$ -dependence algebra is dominated by the cutoff radii  $r_N$  (related to the sizes of the nuclei), and by the power series solutions for  $P_{n\kappa}$  and  $Q_{n\kappa}$  at the origin [32]. The power series coefficients for  $P_{n\kappa}$  and  $Q_{n\kappa}$  depend on the nuclear potential (again related to the sizes of the nuclei), and are constrained by orthogonality of the one-electron functions with the same symmetry. The dominant contributions to the matrix elements of the  $\hat{H}_{int}$  operators come from the valence  $ns^2$  orbitals in the ground state, and from the lowest  $np_{1/2}$  and  $np_{3/2}$  orbitals in the excited states.

The upper graph in the Fig. 3 shows the coefficient  $p_0$  of the lowest order polynomial in the series expansion at the origin of the large component  $P$  of the radial function of the valence orbitals ( $ns$ ,  $np_{1/2}$ ,  $np_{3/2}$ ) of the elements from the group 12 (plus beryllium). The quantum number  $n$  assumes the values 2, 4, 5, 6, 7, 8 for Be, Zn, Cd, Hg, Cn, Uhb, respectively. The lower graph in the Fig. 3 shows the atomic EDMs induced by the TPT, PSS, NSM, and eEDM mechanisms, as functions of atomic number  $Z$  for the elements of the group 12 (plus Be). For the purpose of this comparison, all values in Fig. 3 were obtained in the Dirac-Fock approximation, without account of electron correlation effects, and with the extended nuclear model (3). Analogously to the point nucleus case (represented by the equation (8)), the function  $d_{at}(Z)$  is approximately exponential in the range  $60 < Z < 120$ , i.e. for heavy and superheavy elements relevant from the point of view of the EDM searches. Both graphs in Fig. 3 show similar  $Z$ -dependencies as those in Figure 1, i. e. the polynomial shape up to about  $Z = 60$ , then approximately exponential in the range  $60 < Z < 120$ , and eventually the exponential approximation breaks down near the end of the extended Periodic Table of Elements [59, 75] at  $Z = 173$ . When comparing the shapes of the curves in the upper and lower graphs, one has to bear in mind that radial integrals in matrix elements of the  $\hat{H}_{int}$  operators involve valence  $ns^2$  orbitals in the ground state, and  $np_{1/2}$  and  $np_{3/2}$  orbitals in the excited states. The apparent similarity of the  $np_{1/2}$  and  $np_{3/2}$  curves in the upper graph and the four curves in the lower graph is a numerical confirmation of the dominant role of power series coefficients in the matrix element of the  $\hat{H}_{int}$  operators, as well as of the proportionality relations between matrix elements, established in [21]. Beryllium does not belong to

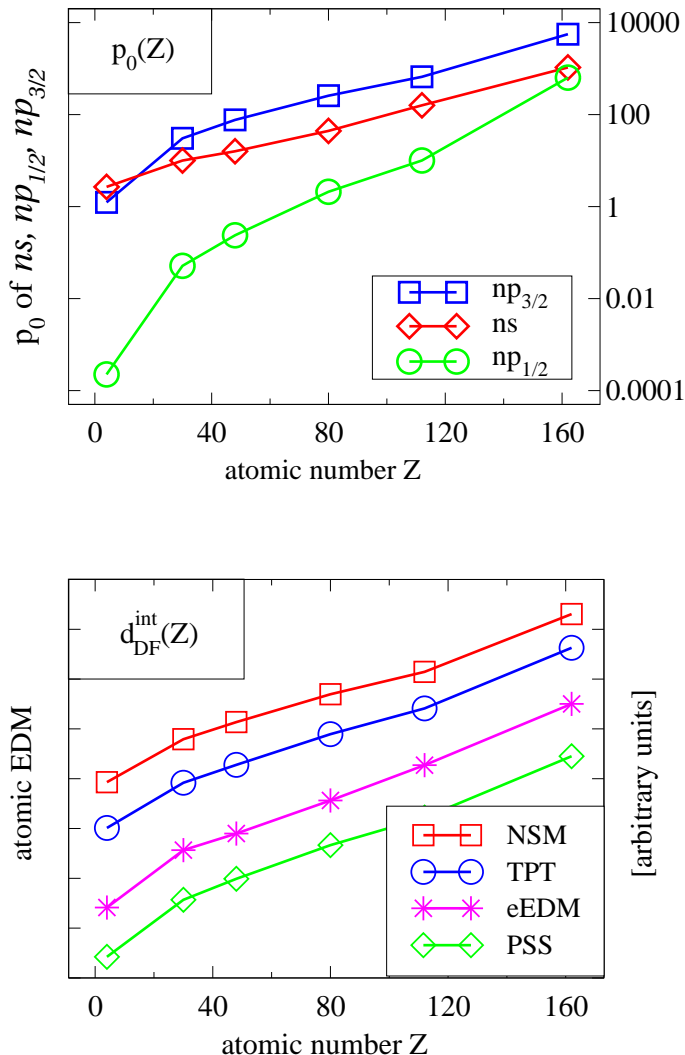


FIG. 3: (Color online) Upper: power series coefficients  $p_0$  of valence orbitals as functions of atomic number  $Z$ . Blue squares =  $np_{3/2}$ ; red diamonds =  $ns$ ; green circles =  $np_{1/2}$ ;  $n = 2, 4, 5, 6, 7, 8$  for Be, Zn, Cd, Hg, Cn, Uhb, respectively. Lower: atomic EDM (in arbitrary units on logarithmic scale) induced by NSM (red squares), TPT (blue circles), eEDM (magenta stars), and by PSS (green diamonds), as a function of atomic number  $Z$ . All lines in both graphs are drawn only for the guidance of the eyes. See text for details.

the group 12 (which results in the visible deviation of Be from the fitted function) but was included in Fig. 3 to indicate that the dominant role of power series coefficients, as well as the proportionality relations [21], are not limited to one group of elements. The other deviations from linearity in the Figure 3 are induced by electron correlation effects, whose contributions differ from element to element due to shell rearrangements.

## IX. CONCLUSIONS

Electric dipole moments (EDMs) have not yet been detected experimentally. The experimental searches have been going on for the last 50 years, and the role of theory is not only to provide the limits on the fundamental parameters, but also to guide the experimentalists to atoms, molecules, and other systems with suitable enhancement factors. Experimentalists need to know (order of magnitude of) enhancement factors before they set up their apparatus to detect EDM in a new species [77]. The present paper is intended to present the calculations of EDMs, carried out with the multiconfiguration Dirac-Hartree-Fock theory, of a superheavy element  $^{285}_{112}\text{Cn}$ . The main conclusion of the present paper is the suggestion for setting up an EDM experiment on a superheavy element, which would result in an order of magnitude increase of sensitivity, compared to a homologous heavy element. Such homologous pairs include (but are not limited to) Yb–No, Hg–Cn, Tl–E113, Po–Lv, At–E117, Rn–E118, Fr–E119, Ra–E120. If the exponential  $Z$ -dependence derived in the present paper is assumed for all above homologous pairs, an increase of sensitivity by a factor 8-30 should be expected. The best limit on the EDM of a diamagnetic atom comes from  $^{199}\text{Hg}$ , for which  $d(^{199}\text{Hg}) < 3.1 \times 10^{-29} e\cdot\text{cm}$  (95% C.L.) has been reported [78]. Our calculations indicate that for the Hg–Cn pair the increase of sensitivity would be 57.5/4.8, 236.9/17.0, 17.6/2.2, and 299.7/10.0 for TPT, PSS, NSM, and eEDM, respectively. Over the last 50 years the precision of EDM experiments has been improving by about an order of magnitude per decade [2, 18, 78–81]. On this timescale an experiment on Cn would be equivalent to time travel into the future over a distance of about ten to twenty years.

We are of course aware of the fact that an EDM experiment on a short-lived superheavy element is impractical at this time. However, the techniques for trapping atoms [82, 83], controlling quantum systems [84, 85], and performing spectroscopic investigations of radioactive [86] and superheavy elements [87] advance rapidly. At the same time the quest for the superheavy island of stability continues [54, 88], and sooner or later one may expect a breakthrough of laser spectroscopic methods into the realm of superheavy elements [87].

The EDM experiments with superheavy elements, if ever becoming feasible, would probably constitute the final frontier for atomic tests of violation of parity ( $P$ ) and time reversal ( $T$ ) symmetries. In recent years the molecular avenue promises to become more competitive in the EDM searches. The advantages of molecular eEDM experiments is in the large values of the effective electric field, several orders of magnitude higher than those in atoms [17, 18, 89]. Current progress in cooling and trapping molecules [90–94], as well as molecular ions [95, 96], may soon allow to increase coherence times and improve population control in molecular experiments, which might translate into a significant advantage of molecular

experiments over atomic ones.

While an EDM experiment on a short-lived superheavy element is impractical at this time, still less practical would be an experiment on a superheavy molecule. However, when molecular EDM experiments become feasible, one may also envisage making, trapping, and eventually performing spectroscopy of superheavy molecules. It is difficult to say what is impossible, for the dream of yesterday is the hope of today and the reality of tomorrow [97].

### Acknowledgments

LR thanks for the HPC resources provided by the ITOAC of Vilnius University. JB, GG, PJ acknowl-

edge the support from the Polish Ministry of Science and Higher Education (MNiSW) in the framework of the grant No. N N202 014140 awarded for the years 2011-2016. JB acknowledges the support from the European Regional Development Fund in the framework of the Polish Innovation Economy Operational Program (contract no. POIG.02.01.00-12-023/08). PJ acknowledges financial support from the Swedish Research Council under the Grant 2015-04842.

- 
- [1] I. B. Khriplovich and S. K. Lamoreaux, *CP Violation Without Strangeness* (Springer, Berlin, 1997).
- [2] K. Jungmann, *Ann. Phys.* **525**, 550564 (2013).
- [3] C. S. Wu, E. Ambler, R. W. Hayward, D. D. Hoppes, and R. P. Hudson, *Phys. Rev.* **105**, 1413 (1957).
- [4] R. L. Garwin, L. M. Lederman, and M. Weinrich, *Phys. Rev.* **105**, 1415 (1957).
- [5] J. I. Friedman and V. L. Telegdi, *Phys. Rev.* **106**, 1290 (1957).
- [6] J. H. Christenson, J. W. Cronin, V. L. Fitch, and R. Turlay, *Phys. Rev. Lett.* **13**, 138 (1964).
- [7] V. A. Kostelecky and N. Russell, *Rev. Mod. Phys.* **83**, 1 (2011).
- [8] A. Angelopoulos, A. Apostolakis, E. Aslanides, G. Backenstoss, P. Bargassa, O. Behnke, A. Benelli, V. Bertin, F. Blanc, P. Bloch, P. Carlson, M. Carroll, E. Cawley, S. Charalambous, M. Chertok, M. Danielsson, M. Dejardin, J. Derre, A. Ealet, C. Eleftheriadis, L. Faravel, W. Fetscher, M. Fidecaro, A. Filipčić, D. Francis, J. Fry, E. Gabathuler, R. Gamet, H.-J. Gerber, A. Go, A. Haselden, P. Hayman, F. Henry-Couannier, R. Hollander, K. Jon-And, P.-R. Kettle, P. Kokkas, R. Kreuger, R. L. Gac, F. Leimgruber, I. Mandić, N. Manthos, G. Marel, M. Mikuž, J. Miller, F. Montanet, A. Muller, T. Nakada, B. Pagels, I. Papadopoulos, P. Pavlopoulos, A. Policarpo, G. Polivka, R. Rickenbach, B. Roberts, T. Ruf, C. Santoni, M. Schäfer, L. Schaller, T. Schietinger, A. Schopper, L. Tauscher, C. Thibault, F. Touchard, C. Touramanis, C. V. Eijk, S. Vlachos, P. Weber, O. Wigger, M. Wolter, D. Zavrtnik, and D. Zimmerman (CPLEAR Collaboration), *Phys. Lett. B* **444**, 43 (1998).
- [9] L. Wolfenstein, *Int. J. Mod. Phys. E* **08**, 501 (1999).
- [10] J. Bernabeu, A. D. Domenico, and P. Villanueva-Perez, *Nucl. Phys. B* **868**, 102 (2013).
- [11] J. P. Lees *et al.* (The BABAR Collaboration), *Phys. Rev. Lett.* **109**, 211801 (2012).
- [12] N. Cabibbo, *Phys. Rev. Lett.* **10**, 531 (1963).
- [13] M. S. Sozzi, *Discrete Symmetries and CP Violation. From Experiment to Theory* (Oxford University Press, Oxford, 2008).
- [14] C. A. Baker, D. D. Doyle, P. Geltenbort, K. Green, M. G. D. van der Grinten, P. G. Harris, P. Iaydjiev, S. N. Ivanov, D. J. R. May, J. M. Pendlebury, J. D. Richardson, D. Shiers, and K. F. Smith, *Phys. Rev. Lett.* **97**, 131801 (2006).
- [15] B. C. Regan, E. D. Commins, C. J. Schmidt, and D. DeMille, *Phys. Rev. Lett.* **88**, 071805 (2002).
- [16] W. C. Griffith, M. D. Swallows, T. H. Loftus, M. V. Romalis, B. R. Heckel, and E. N. Fortson, *Phys. Rev. Lett.* **102**, 101601 (2009).
- [17] J. J. Hudson, D. M. Kara, I. J. Smallman, B. E. Sauer, M. R. Tarbutt, and E. A. Hinds, *Nature* **473**, 493 (2011).
- [18] T. A. C. J. Baron, W. C. Campbell, D. DeMille, J. M. Doyle, G. Gabrielse, Y. V. Gurevich, P. W. Hess, N. R. Hutzler, E. Kirilov, I. Kozyryev, B. R. O’Leary, C. D. Panda, M. F. Parsons, E. S. Petrik, B. Spaun, A. C. Vutha, and A. D. West (The ACME Collaboration), *Science* **343**, 269 (2014).
- [19] J. S. M. Ginges and V. V. Flambaum, *Phys. Rep.* **397**, 63 (2004).
- [20] B. L. Roberts and W. J. Marciano, eds., *Advanced Series on Directions in High Energy Physics*, Vol. 20 (World Scientific, Singapore, 2009).
- [21] V. A. Dzuba, V. V. Flambaum, and C. Harabati, *Phys. Rev. A* **84**, 052108 (2011).
- [22] H. Gould and C. T. M. Jr., “Position paper: Electric dipole moment experiments,” <http://fsnutown.phy.ornl.gov/fsnuweb/index.html> (28-29 Sep 2014).
- [23] M. D. Swallows, T. H. Loftus, W. C. Griffith, B. R. Heckel, and E. N. Fortson, *Phys. Rev. A* **87**, 012102 (2013).
- [24] R. Eichler, N. V. Aksenov, A. V. Belozarov, G. A. Bozhikov, V. I. Chepigin, S. N. Dmitriev, R. Dressler, H. W. Gäggeler, V. A. Gorshkov, F. Haenssler, M. G. Itkis, A. Laube, V. Y. Lebedev, O. N. Malyshev, Y. T. Oganessian, O. V. Petrushkin, D. Pigué, P. Rasmussen, S. V. Shishkin, A. V. Shutov, A. I. Svirikhin, E. E. Tereshatov, G. K. Vostokin, M. Wegrzecki, and A. V. Yerein, *Nature* **447**, 72 (2002).
- [25] R. C. Barber, H. W. Gäggeler, P. J. Karol, H. Nakahara, E. Vardaci, and E. Vogt, *Pure Appl. Chem.* **81**, 13311343 (2009).
- [26] K. G. Dyall, I. P. Grant, C. T. Johnson, F. A. Parpia, and E. P. Plummer, *Comput. Phys. Commun.* **55**, 425

- (1989).
- [27] P. Jönsson, G. Gaigalas, J. Bieroń, C. Froese Fischer, and I. P. Grant, *Comput. Phys. Commun.* **184**, 2197 (2013).
- [28] B. J. McKenzie, I. P. Grant, and P. H. Norrington, *Comput. Phys. Commun.* **21**, 233 (1980).
- [29] F. A. Parpia, C. Froese Fischer, and I. P. Grant, *Comput. Phys. Commun.* **94**, 249 (1996).
- [30] I. P. Grant, *Comput. Phys. Commun.* **84**, 59 (1994).
- [31] P. Jönsson, X. He, and C. Froese Fischer, *Comput. Phys. Commun.* **176**, 597 (2007).
- [32] I. P. Grant, *Relativistic Quantum Theory of Atoms and Molecules: Theory and Computation* (Springer, New York, 2007).
- [33] L. Radziūtė, G. Gaigalas, P. Jönsson, and J. Bieroń, *Phys. Rev. A* **90**, 012528 (2014).
- [34] J. Bieroń, C. Froese Fischer, P. Indelicato, P. Jönsson, and P. Pyykkö, *Phys. Rev. A* **79**, 052502 (2009).
- [35] J. Bieroń, C. Froese Fischer, S. Fritzsche, G. Gaigalas, I. P. Grant, P. Indelicato, P. Jönsson, and P. Pyykkö, *Phys. Scr.* **90**, 054011 (2015).
- [36] L. Radziūtė, G. Gaigalas, D. Kato, P. Jönsson, P. Rynkun, S. Kučas, V. Jonauskas, and R. Matulianec, *J Quant Spectrosc Radiat Transf* **152**, 94 (2015).
- [37] G. Gaigalas, Z. Rudzikas, and C. Froese Fischer, *J. Phys. B: At. Mol. Opt. Phys.* **30**, 3747 (1997).
- [38] R. D. Cowan and J. E. Hansen, *J. Opt. Soc. Am.* **71**, 60 (1981).
- [39] P. Syty, J. Sienkiewicz, L. Radziūtė, G. Gaigalas, and J. Bieroń, (2016), work in progress.
- [40] U. Fano and J. W. Cooper, *Rev. Mod. Phys.* **40**, 441507 (1965).
- [41] V. A. Dzuba, V. V. Flambaum, and S. G. Porsev, *Phys. Rev. A* **80**, 032120 (2009).
- [42] A.-M. Mårtensson-Pendrill, *Phys. Rev. Lett.* **54**, 1153 (1985).
- [43] K. V. P. Latha, D. Angom, R. J. Chaudhuri, B. P. Das, and D. Mukherjee, *J. Phys. B: At. Mol. Opt. Phys.* **41**, 035005 (2008).
- [44] K. V. P. Latha, D. Angom, B. P. Das, and D. Mukherjee, *Phys. Rev. Lett.* **103**, 083001 (2009).
- [45] V. A. Dzuba, V. V. Flambaum, J. S. M. Ginges, and M. G. Kozlov, *Phys. Rev. A* **66**, 012111 (2002).
- [46] V. A. Dzuba, V. V. Flambaum, and J. S. M. Ginges, *Phys. Rev. A* **76**, 034501 (2007).
- [47] A.-M. Mårtensson-Pendrill and P. Öster, *Phys. Scr.* **36**, 444 (1987).
- [48] A. Kramida, Yu. Ralchenko, J. Reader, and NIST ASD Team, <http://physics.nist.gov/asd>.
- [49] G. Gaigalas, T. Žalandauskas, and Z. Rudzikas, *Atomic Data Nucl. Data Tab.* **84**, 99 (2003).
- [50] G. Gaigalas, T. Žalandauskas, and S. Fritzsche, *Comput. Phys. Commun.* **157**, 239 (2004).
- [51] Y. J. Yu, J. G. Li, C. Z. Dong, X. B. Ding, S. Fritzsche, and B. Fricke, *Eur. Phys. J. D* **44**, 51 (2007).
- [52] T. H. Dinh, V. A. Dzuba, and V. V. Flambaum, *Phys. Rev. A* **78**, 062502 (2008).
- [53] R. Smolańczuk, *Phys. Rev. C* **56**, 812 (1997).
- [54] V. Zagrebaev, A. Karpov, and W. Greiner, *J. Phys.: Conf. Ser.* **420**, 012001 (2013).
- [55] <http://www.nndc.bnl.gov/nudat2>.
- [56] B. Graner, Y. Chen, E. G. Lindahl, and B. R. Heckel, (2016), arXiv:1601.04339 [physics.atom-ph] .
- [57] B. Fricke, W. Greiner, and J. T. Waber, *Theoret. Chim. Acta* **21**, 235 (1971).
- [58] R. A. Penneman, J. B. Mann, and C. K. Jørgensen, *Chem. Phys. Lett.* **8**, 321 (1971).
- [59] P. Pyykkö, *Phys. Chem. Chem. Phys.* **13**, 161 (2011).
- [60] C. Froese Fischer, T. Brage, and P. Jönsson, *Computational Atomic Structure. An MCHF Approach* (Institute of Physics Publishing, Bristol and Philadelphia, 1997).
- [61] D. Layzer, *Ann. Phys* **8**, 271 (1959).
- [62] D. Layzer, Z. Horák, M. N. Lewis, and D. P. Thompson, *Ann. Phys* **29**, 101 (1964).
- [63] B. Edlén, “Handbuch der physik,” (Springer, Berlin, 1964) p. 80.
- [64] R. D. Cowan, *The Theory of Atomic Structure and Spectra* (University of California Press, Ltd, Berkeley, 1981).
- [65] W. L. Wiese and A. W. Weiss, *Phys. Rev.* **175**, 50 (1968).
- [66] M. A. Bouchiat and C. Bouchiat, *J. de Physique* **35**, 899 (1974).
- [67] M. A. Bouchiat and C. C. Bouchiat, *Phys.Lett.* **48B**, 111 (1974).
- [68] M. A. Bouchiat and C. Bouchiat, *J. de Physique* **36**, 493 (1975).
- [69] O. P. Sushkov, V. V. Flambaum, and I. B. Khriplovich, *Zh. Eksp. Teor. Fiz.* **87**, 1521 (1984).
- [70] I. B. Khriplovich, *Parity Nonconservation in Atomic Phenomena* (Gordon and Breach, New York, 1991).
- [71] V. V. Flambaum and J. S. M. Ginges, *Phys. Rev. A* **65**, 032113 (2002).
- [72] J. W. Rohlfs, *Modern Physics from  $\alpha$  to  $Z^0$*  (Wiley, 1994).
- [73] W. Greiner, *Relativistic Quantum Mechanics — Wave Equations* (Springer-Verlag, Berlin Heidelberg, 1990).
- [74] W. Greiner, *Quantum Electrodynamics* (Springer-Verlag, Berlin Heidelberg, 1994).
- [75] P. Indelicato, J. Bieroń, and P. Jönsson, *Theor. Chem. Acc.* **129**, 495 (2011).
- [76] I. Goidenko, I. Tupitsyn, and G. Plunien, *Eur. Phys. J. D* **45**, 171177 (2007).
- [77] K. Jungmann, *Ann. Phys.* **525**, 550564 (2013).
- [78] W. C. Griffith, M. D. Swallows, T. H. Loftus, M. V. Romalis, B. R. Heckel, and E. N. Fortson, *Phys. Rev. Lett.* **102**, 101601 (2009).
- [79] J. M. Amini, C. T. Munger, Jr., and H. Gould, *Phys. Rev. A* **75**, 063416 (2007).
- [80] M. V. Romalis, W. C. Griffith, J. P. Jacobs, and E. N. Fortson, *Phys. Rev. Lett.* **86**, 2505 (2001).
- [81] M. D. Swallows, T. H. Loftus, W. C. Griffith, B. R. Heckel, and E. N. Fortson, *Phys. Rev. A* **87**, 012102 (2013).
- [82] C. E. Wieman, D. E. Pritchard, and D. J. Wineland, *Rev. Mod. Phys.* **71**, S253 (1999).
- [83] S. De, U. Dammalapati, and L. Willmann, *Phys. Rev. A* **91**, 032517 (2015).
- [84] D. J. Wineland, *Rev. Mod. Phys.* **85**, 1103 (2013).
- [85] A. D. Ludlow, M. M. Boyd, and J. Ye, *Rev. Mod. Phys.* **87**, 637 (2015).
- [86] R. H. Parker, M. R. Dietrich, M. R. Kalita, N. D. Lemke, K. G. Bailey, M. N. Bishof, J. P. Greene, R. J. Holt, W. Korsch, Z.-T. Lu, P. Mueller, T. P. O’Connor, and J. T. Singh, *Phys. Rev. Lett.* **114**, 233002 (2015).
- [87] B. Cheal and K. T. Flanagan, *J. Phys. G: Nucl. Part. Phys.* **37**, 113101 (2010).
- [88] Y. Oganessian, *J. Phys.: Conf. Ser.* **337**, 012005 (2012).
- [89] S. Sasmal, H. Pathak, M. K. Nayak, N. Vaval, and S. Pal, *The Journal of Chemical Physics* **144**, 124307 (2016).

- [90] E. B. Norrgard, D. J. McCarron, M. H. Steinecker, M. R. Tarbutt, and D. DeMille, *Phys. Rev. Lett.* **116**, 063004 (2016).
- [91] A. Prehn, M. Ibrügger, R. Glöckner, G. Rempe, and M. Zeppenfeld, *Phys. Rev. Lett.* **116**, 063005 (2016).
- [92] T. A. Isaev and R. Berger, *Phys. Rev. Lett.* **116**, 063006 (2016).
- [93] C. D. Panda, B. R. OLeary, A. D. West, J. Baron, P. W. Hess, C. Hoffman, E. Kirilov, C. B. Overstreet, E. P. West, D. DeMille, J. M. Doyle, and G. Gabrielse, (2016), arXiv:1603.07707v1 [physics.atom-ph] .
- [94] T. Fleig, M. K. Nayak, and M. G. Kozlov, *Phys. Rev. A* **93**, 012505 (2016).
- [95] A. E. Leanhardt, J. L. Bohn, H. Loh, P. Maletinsky, E. R. Meyer, L. C. Sinclair, R. P. Stutz, and E. A. Cornell, *J. Mol. Spectrosc.* **270**, 1 (2011).
- [96] D. N. Gresh, K. C. Cossel, Y. Zhou, J. Ye, and E. A. Cornell, *J. Mol. Spectrosc.* **319**, 1 (2016).
- [97] Attributed to Robert H. Goddard.